ELSEVIER

Journal of Chromatography A, 734 (1996) 183–194

JOURNAL OF CHROMATOGRAPHY A

Adsorption isotherms in protein chromatography Combined influence of protein and salt concentration on adsorption isotherm

Oliver Kaltenbrunner, Alois Jungbauer*

Institute of Applied Microbiology, University of Agriculture, Forestry and Biotechnology, Nussdorferlände 11, A-1190 Vienna, Austria

Abstract

The distribution coefficient (K) of a protein in ion-exchange chromatography is dependent on the protein and salt concentration in the mobile phase. Conventional isotherms only describe the relationship between the mobile phase and stationary phase concentrations of the protein, the influence of salt being neglected. In this paper, the dependence of K on salt is described by transition functions [$\varphi(I)$] such as logistic dose response and hyperbolic tangent functions. The relationship between K and protein concentration is described by conventional isotherms; the K value is considered as the first derivative of the isotherm, or as the ratio between concentrations in the mobile and stationary phases. The stationary phase concentration can be expressed as a function of the mobile phase concentration. Combinations of these functions with transition functions can be used to approximate the binding characteristics of a protein dependent on protein and salt concentration.

Keywords: Adsorption isotherms; Distribution coefficients; Peak shape; Proteins; Albumin

1. Introduction

Under non-linear conditions, the exact knowledge of the adsorption isotherm of proteins is a prerequisite for the simulation and prediction of peak profiles. Over many years, numerous adsorption isotherms have been reported [1–9], derived from different experimental models concerning the adsorbate and the adsorbent. In most cases, the binding of proteins on ion exchangers has not been the basis for establishing these mathematical relationships. Nevertheless, these relationships have been successfully translated into protein chromatography using ion exchangers [10]. For modes other than isocratic separation, the influence of salt (more correctly, the ionic strength) must also be taken into account. Yamamoto et al. [11] approximated that the distribution coefficient (K) was dependent on salt by a simple power function:

$$K(I) = \alpha I^{\beta} + K_{crt} \quad (1)$$

where I is the ionic strength, α and β are parameters with limited physical meaning and K_{crt} is the distribution coefficient at very high salt concentration (when the protein is not bound to the ion exchanger). Using the stoichiometric

* Corresponding author.

0021-9673/96/$15.00 © 1996 Elsevier Science B.V. All rights reserved
SSDI 0021-9673(95)01149-8

displacement model, this distribution coefficient is also described by a power function [12]. This equation contains several parameters, such as the exact equilibrium concentration of the free and bound protein and salt. Because equilibria data are not easily accessible, the practical application of such an equation is limited. On the other hand, the extension of existing equations for the distribution coefficient gives a more appropriate description of the practical situation. The assignment of the parameters to physical meaning is no longer possible.

In this paper, we describe a set of equations to fit the experimental distribution coefficients. These equations are inserted in simple mass balance equations to identify their influence on a simulated peak profile.

2. Theory

Considering constant I, the distribution coefficient (K) of a protein between the ion exchanger and the mobile phase can be described by

$$K(C_m) = \frac{dC_s}{dC_m} \tag{2}$$

where C_s is the stationary phase concentration and C_m is the mobile phase concentration of a protein (after equilibrium is obtained). If I is constant, Eq. 2 is equivalent to the first derivative of the function describing the adsorption isotherm. Further, the dependence of the distribution coefficient on the salt concentration can be approximated by a logistic dose response function [13]:

$$\varphi(I) = \frac{a}{1 + \left(\frac{I}{b}\right)^c} = \frac{a}{\Phi(I)} \tag{3}$$

where a denotes the amplitude, b the inflection point and c the slope of the transition. This function can also be extended to an asymmetric logistic dose–response function by introducing a symmetry parameter (d) as an exponent in the denominator:

$$\varphi(I) = \frac{a}{\left[1 + \left(\frac{I}{b}\right)^c\right]^d} \tag{4}$$

Further, the transition function can be described by a hyperbolic tangent function such as

$$\varphi(I) = a \cdot \frac{1 + \tanh[-b(I-c)]}{2} \tag{5}$$

where a denotes the amplitude, b the slope and c the transition centre. Similarly to the logistic functions, this hyperbolic tangent function can also be extended to an asymmetric function by introducing a symmetry parameter (d) as an exponent:

$$\varphi(I) = a \cdot \frac{\{1 + \tanh[-b(I-c)]\}^d}{2} \tag{6}$$

K, dependent on I and C_m, can be fitted by a function $\Gamma(I, C_m)$:

$$\Gamma(I, C_m) = \varphi(I)\frac{dC_s}{dC_m} \tag{7}$$

A further simplification can be achieved by replacing the derivation Eq. 2 by a simple ratio:

$$K(C_m) = \frac{C_s}{C_m} \tag{8}$$

The stationary phase concentration is expressed by

$$C_s = f(C_m) \tag{9}$$

This equation is a general form of an adsorption isotherm. For this simplified case, the function for fitting the experimental data is now written as

$$\Gamma(I, C_m) = \varphi(I)\frac{f(C_s)}{C_m} \tag{10}$$

These functions $\Gamma(I, C_m)$ (Eqs. 7 and 10) can be used to fit the experimental data $K(I, C_m)$. A list of functions for different adsorption isotherms is given in the Appendix.

3. Experimental

3.1. Chromatographic system

Two P-3500 high-performance pumps (Pharmacia Biotech, Uppsala, Sweden) were controlled by an LCC-500 Plus liquid chromatography controller (Pharmacia Biotech). The column effluent was monitored by UV-M monitor (Pharmacia Biotech) at 280 nm and a conductivity monitor (Pharmacia Biotech). The analogue signals were transferred to a PE Nelson 900 Series interface and stored digitally by Model 2600 Rev. 4.1 chromatography software (Nelson Analytical, Cupertino, CA, USA). Samples were injected by a PMV-7 motor valve (Pharmacia Biotech, Uppsala, Sweden) or, in the case of frontal analysis, the sample was loaded by a P-3500 pump.

3.2. Sorbent

Q-HyperD-F anion exchanger was obtained by BioSepra (Marlborough, MA, USA).

3.3. Buffers

For equilibration, 10 m*M* Tris–HCl buffer (pH 8.0) was used. For elution and regeneration, 10 m*M* Tris–HCl buffer (pH 8.0)–1 *M* NaCl was used. Equilibration and elution buffers were blended to obtain linear gradients.

3.4. Samples

As a model protein, highly purified bovine serum albumin (Sigma, St. Louis, MO, USA; Catalogue No. A-6918) was used. The lyophilized powder was reconstituted in equilibration buffer and prepared freshly for each set of experiments.

3.5. Numerical treatment of data

Raw data from the chromatograms were exported from the Nelson data acquisition software to all other programs as tab-delimited textfiles. In isocratic and linear gradient experiments, these data were fitted with exponential modified Gaussian peaks. Fitting was carried out by using the software Peak Fit Version 3.0 (Jandel Scientific, San Rafael, CA, USA). The parameters for the K values were estimated using the computer program Table Curve 3D Version 1.05 (Jandel Scientific) and approximation of $K(I, C)$ was carried out according to

$$\sum_{c=1}^{N} [\Gamma(I_c, C_c) - K(I_c, C_c)]^2 = \min \tag{11}$$

4. Results

4.1. Experimental determination of distribution coefficient

The distribution coefficient was determined by frontal analysis [adsorbing BSA on the anion exchanger Q-HyperD (F)]. K values were derived from a 100% saturated column (Fig. 1). Then the sample volume corresponding to the adsorbed amount of protein was calculated by numerical integration of the detector response. The area obtained from the filled column was subtracted from that for the empty column. This area is equivalent to the sample volume (V_{BTC}) which was required to saturate the column. The distribution coefficients (K) were calculated by

$$K = \frac{V_{BTC}}{(1 - \varepsilon)V_t} \tag{12}$$

K values were plotted against protein and salt concentration in the mobile phase (Fig. 2). The

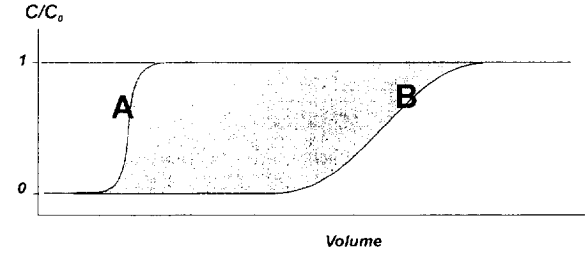

Fig. 1. Determination of K values by breakthrough curves using 100% column capacity. (A) Breakthrough curve without column; (B) breakthrough curve with column.

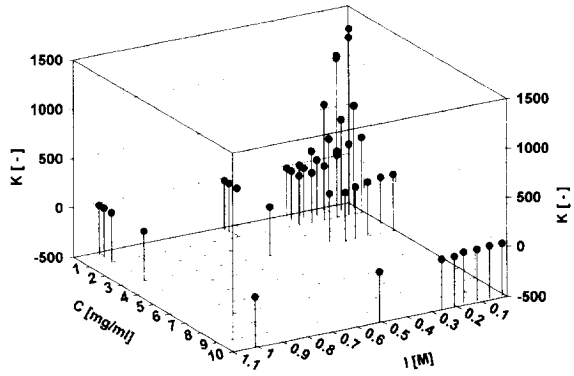

Fig. 2. Distribution coefficient (K) of BSA on Q-HyperD (F) obtained by frontal analysis.

three-dimensional fit of the data by a function derived from a Toth isotherm combined with an asymmetric logistic dose–response function is shown as an example (Fig. 3).

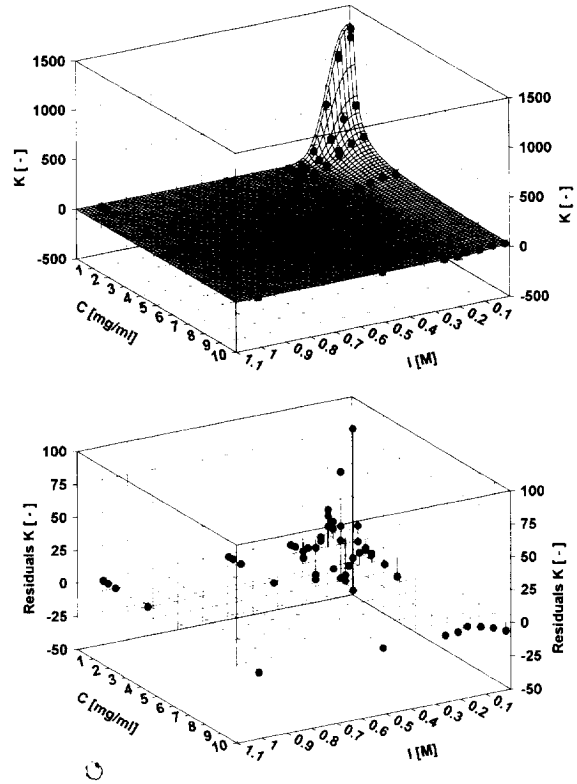

Fig. 3. (Top) Approximation of the K values of BSA on Q-HyperD (F) by Eq. A48; (bottom) residuals between experimental data and approximated data.

Because the K value corresponds to the slope of the adsorption isotherm, $K(I, C)$ can be expressed by two different concepts: it can be treated as a differential quotient or as the ratio between C_s and C_m. For demonstration of the applicability of the different concepts, the equations for the distribution coefficients were inserted in a simple mass balance equation, then explicit solutions for C_m were searched.

4.2. Differential quotient

In this case, $K(I, C_m)$ is considered as the first derivative of the adsorption isotherm. Eq. 7 can be inserted in a simple mass balance equation (as described previously [13]):

$$C_{m_{(n)(t)}} \cdot \frac{V_0}{N} + C_{m_{(n)(t)}} \cdot \frac{V_t - V_0}{N} \cdot K_{(n)(t)} = C_{m_{(n-1)(t-1)}} \cdot \frac{V_0}{N} + C_{m_{(n)(t-1)}} \cdot \frac{V_t - V_0}{N} \cdot K_{(n)(t-1)} \quad (13)$$

where n and t (in parentheses) denote the space and the time increment under consideration, respectively. All terms on the right-hand side of Eq. 13 are defined from the previous step of the calculation. $C_{m(n)(t)}$ is the unknown concentration of the substance of interest and $K_{(n)(t)}$ is only accessible when $C_{m(n)(t)}$ is known. To demonstrate the difficulties that arise, the equation corresponding to the first derivatization of the Langmuir adsorption isotherm:

$$K(n)(t) = \frac{a}{\Phi(I)(1 + dC_m)^2} \quad (14)$$

is inserted into Eq. 13 to substitute $K_{(n)(t)}$. The solution of Eqs. 13 and 14 with respect to C_m leads to a cubic equation:

$$AC_m^3 + BC_m^2 + CC_m + D = 0 \quad (15)$$

where

$$A = d^2\Phi(I)V_0 \quad (15a)$$

$$B = -d\Phi(I)\{[C_{m_{t-1}}V_0 + C_{s_{t-1}}(V_t - V_0)]d - 2V_0\} \quad (15b)$$

$$C = a(V_t - V_0) - \Phi(I)\{2[C_{m_{t-1}}V_0 + C_{s_{t-1}} \times (V_t - V_0)]d - V_0\} \quad (15c)$$

$$D = -[C_{m_{t-1}}V_0 + C_{s_{t-1}}(V_t - V_0)\Phi(I) \quad (15d)$$

where $C_{m_{t-1}}$ and $C_{s_{t-1}}$ are the mobile and the stationary phase concentrations of the previous calculation increment, respectively. This cubic equation possesses three explicit solutions for C_m in the range of interest, denoted C_{m_1}, C_{m_2} and C_{m_3}:

$$C_{m_1} = 2\sqrt{B^2 - 3AC} \cdot \frac{\sin\left(\frac{a \tan \Psi}{3}\right)}{3|A|} - \frac{B}{3A} \quad (16)$$

$$C_{m_2} = -\text{sign } A\sqrt{B^2 - 3AC} \times \left[\sqrt{3} \cdot \frac{\cos\left(\frac{a \tan \Psi}{3}\right)}{3A} + \frac{\sin\left(\frac{a \tan \Psi}{3}\right)}{3A} - \frac{B}{3A}\right] \quad (17)$$

$$C_{m_3} = \text{sign } A\sqrt{B^2 - 3AC} \times \left[\sqrt{3} \cdot \frac{\cos\left(\frac{a \tan \Psi}{3}\right)}{3A} - \frac{\sin\left(\frac{a \tan \Psi}{3}\right)}{3A} - \frac{B}{3A}\right] \quad (18)$$

where

$$\Psi = \sqrt{3} \cdot \frac{27A^2D - 9ABC + 2B^3}{\left[9A(B^2 - 3AC)^{3/2} \times \sqrt{\frac{27A^2D^2 - 2AC(9BD - 2C^2) + B^2(4BD - C^2)}{(3AC - B^2)^3}}\right]} \quad (19)$$

Assuming certain initial conditions of the stationary and mobile phase concentrations, different solutions of C_m are plotted versus I (Fig. 4).

4.3. Distribution coefficient as a ratio between C_s and C_m

This simplification uses a ratio instead of a differential quotient, which yields the following equation:

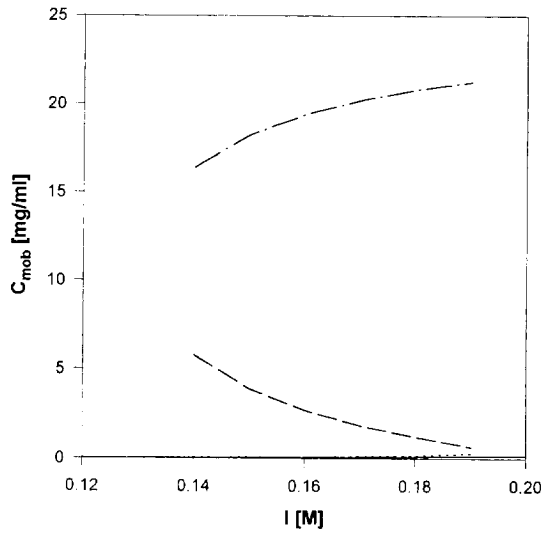

Fig. 4. Starting with defined conditions, the possible values of C_m at the next time point (stepping one time increment further) are plotted. Comparison of the solutions of Eqs. 16 (——), 17 (· · · · ·), 18 (— · —) and 21 (———) assuming a mobile phase concentration of $C_m = 0.2$ mg/ml and a stationary phase concentration $C_s = 20$ mg/ml as the initial conditions of the calculation. $V_0 = 0.467$; $V_t = 1.0$. Parameters for Eqs. 14 and 20 with $\Phi(I)$ replaced according to Eq. 3: $a = 2670.26$; $b = 0.10204$; $c = 4.061$; $d = 2.40388$.

$$K = \frac{a}{\Phi(I)(1 + dC_m)} \quad (20)$$

considering a Langmuir adsorption isotherm. The equations for other isotherms are listed in the Appendix. Insertion of Eq. 20 into Eq. 13 leads to a quadratic equation that forms two solutions for C_m (denoted C_{m_1} and C_{m_2}):

$$C_{m_1} = \frac{\sqrt{B^2 - 4AC} - B}{2A} \quad (21)$$

$$C_{m_2} = -\frac{\sqrt{B^2 - 4AC} + B}{2A} \quad (22)$$

where

$$A = \Phi(I)V_0d \quad (23)$$

$$B = \Phi(I)\{V_0 - d[C_{m_{t-1}}V_0 + C_{s_{t-1}}(V_t - V_0)]\} \quad (24)$$

$$C = \Phi(I)[C_{m_{t-1}}V_0 + C_{s_{t-1}}(V_t - V_0)] \quad (25)$$

This approach is much easier to handle, since only Eq. 21 leads to an explicit solution in the

range of interest. The possible solution of C_m in the positive range is plotted versus I (Fig. 4). Parameters describing the maximum capacity (q_{max}) are compared (Table 1); q_{max} can be derived from the equations in the Appendix. The parameter a always contains q_{max}. In some cases, the parameter also contains additional factors. Equations using Langmuir–Freundlich and Langmuir isotherms do not give reliable values for q_{max}. When considering the case of the Langmuir–Freundlich isotherm, the 95% confidence interval exceeds q_{max} by several orders of magnitude. Deviations of the approximated function from experimental data are exemplified by 2D plots (where protein or salt was kept constant). At low salt concentration, the approximation appears to be more accurate than at higher salt concentrations (Fig. 5A–E).

5. Discussion

In ion-exchange chromatography, the approximation of K values $[K(C, I)]$ by a function $\Gamma(C, I)$ suffers from two fundamental problems. First, the shape of the isotherm changes with the salt concentration in the mobile phase. To achieve reliable parameters for the two dimensions, C and I, the type of the isotherm is kept constant and only q_{max} is made dependent on salt. The drawback of this simplification is clearly visible in (Fig. 5A–E), when the isotherms at 0.21 and 0.06 M salt are compared. At low salt concentration, the bending of the real isotherm is more pronounced than at high concentrations. However, the mathematical model does not allow different shapes of the isotherm. This is the drawback of our models, but we are able to

Table 1
Calculated values for the maximum binding capacity (q_{max}) derived from fit equations, which represent combinations of a number of different adsorption isotherms and different approaches to describe the dependence on salt concentration (I)[a]

$K(C)$	$K(I)$	Freundlich		Langmuir		Langmiur–Freundlich	
		q_{max}	CI 95%	q_{max}	CI 95%	q_{max}	CI 95%
dC_s/dC_m	LDR	*6476.94 ± 2.55 × 10⁶*		**2670.27 ± 219.908**		*2954.55 ± 5.07 × 10⁵*	
dC_s/dC_m	*asym*LDR	*6872.96 ± 1.87 × 10⁶*		**2757.37 ± 167.814**		*3103.25 ± 2.88 × 10⁶*	
dC_s/dC_m	tanh	*7161.53 ± 2.22 × 10⁶*		*2872.71 ± 311.974*		*3237.60 ± 3.17 × 10⁶*	
dC_s/dC_m	*asym*tanh	*1828.96 ± 6.87 × 10⁶*		*225.95 ± 1485.392*		*594.67 ± 9.47 × 10⁵*	
C_s/C_m	LDR	**264.18 ± 16.073**		*1.34 × 10⁷ ± 1.12 × 10¹⁰*		*661034.76 ± 1.76 × 10⁷*	
C_s/C_m	*asym*LDR	**271.64 ± 10.759**		*3.09 × 10⁷ ± 3.85 × 10¹⁰*		*374.91 ± 1.22 × 10⁴*	
C_s/C_m	tanh	**283.58 ± 12.271**		*8.36 × 10⁸ ± 2.71 × 10¹³*		*246047.42 ± 3.88 × 10⁶*	
C_s/C_m	*asym*tanh	*71.91 ± 147.730*		*3.46 × 10⁸ ± 7.11 × 10¹³*		*167.51 ± 1895.65*	
		Jovanovic		Redlich–Peterson		Toth		Temkin	
		q_{max}	CI 95%	q_{max}	CI 95%	q_{max}	CI 95%	q_{max}	CI 95%
dC_s/dC_m	LDR	n.f.[b]		11050.54 ± 9081.513		*2954.55 ± 5.07 × 10⁵*		n.f.	
dC_s/dC_m	*asym*LDR	n.f.		11905.68 ± 6504.901		*3103.25 ± 2.88 × 10⁶*		n.f.	
dC_s/dC_m	tanh	n.f.		12339.27 ± 6762.648		*9475.95 ± 3.18 × 10⁸*		n.f.	
dC_s/dC_m	*asym*tanh	n.f.		*2476.61 ± 6465.409*		*417848 ± 1.11 × 10⁹*		n.f.	
C_s/C_m	LDR	**264.18 ± 16.073**		*5099.41 ± 5256.320*		**264.18 ± 16.073**		*528.82 ± 4.77 × 10⁶*	
C_s/C_m	*asym*LDR	**269.21 ± 7.767**		5600.62 ± 4053.682		**270.71 ± 7.590**		*555.60 ± 6.82 × 10⁵*	
C_s/C_m	tanh	**280.78 ± 9.307**		5935.20 ± 4322.5624		*361.89 ± 1282.642*		n.f.	
C_s/C_m	*asym*tanh	*54.87 ± 135.597*		*1121.23 ± 3327.542*		*174.15 ± 11052.812*		n.f.	

[a] The values are given together with the confidence interval at a confidence level of 95% (CI 95%). Bold numbers indicate a CI 95% smaller than 10% of q_{max} and numbers in italics indicate a CI 95% exceeding q_{max}.
[b] n.f. indicates cases where it was not possible to reach a good fit.

describe K parameters dependent on both protein and salt. The previously described models only deal with one type of isotherm.

Second, the dependence of q_{max} on I cannot be described by a symmetric transition function. This results in the functions becoming more complex and the significance of the parameters may be lost in some cases. For more accurate approximation, the physical significance of the different parameters has to be sacrificed. The K value as a function of salt can be sufficiently described by a logistic dose response function (Eqs. 3 and 4), or a hyperbolic tangent function (Eqs. 5 and 6). Although the mathematical meanings are clearly defined, we are not able to assign physical meanings to the parameters of these functions. Because the shape of the adsorption isotherm changes with salt, all parameters should be made dependent on the salt concentration. In our model, all dependences on

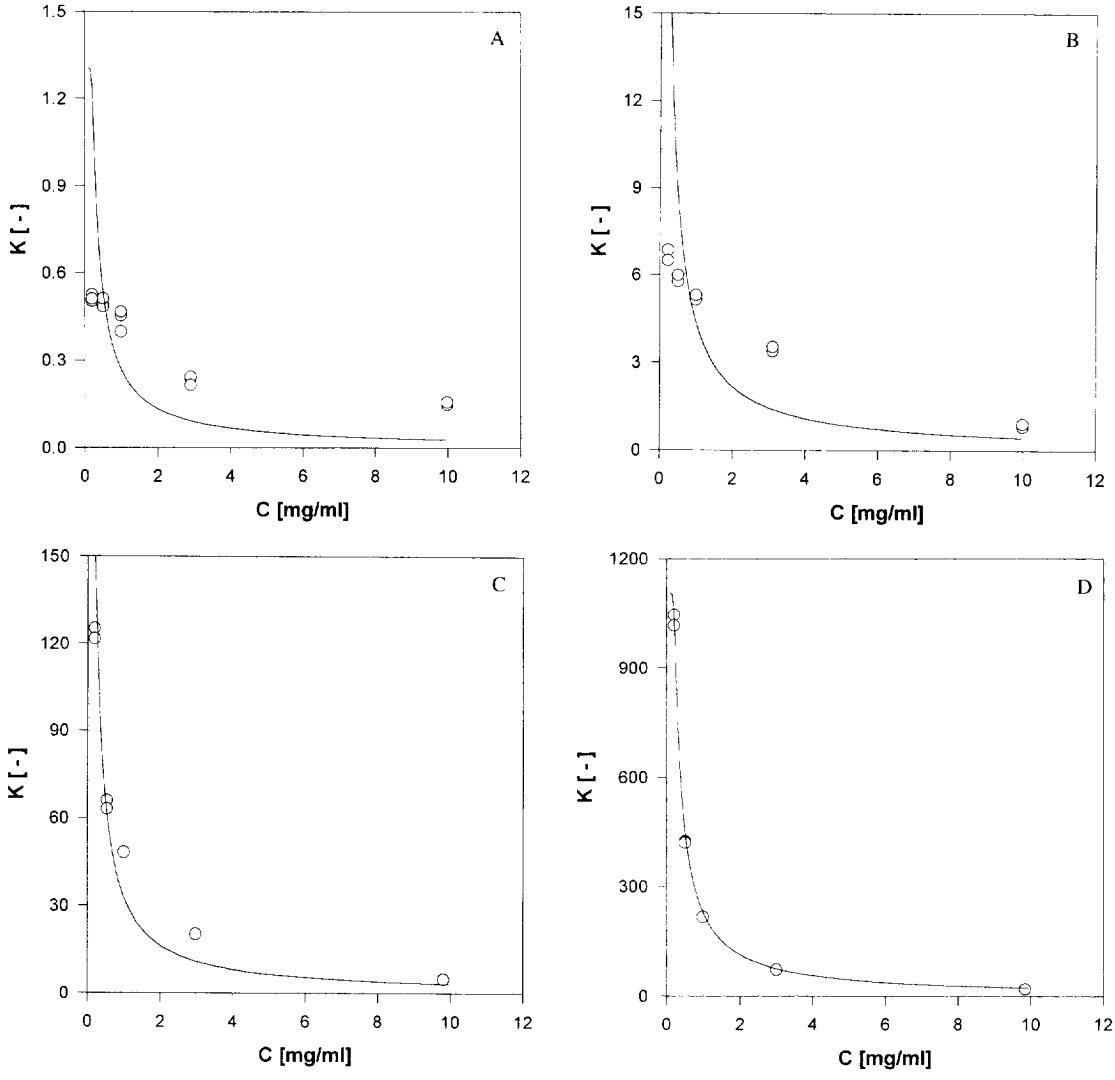

Fig. 5 (*continued on p. 190*).

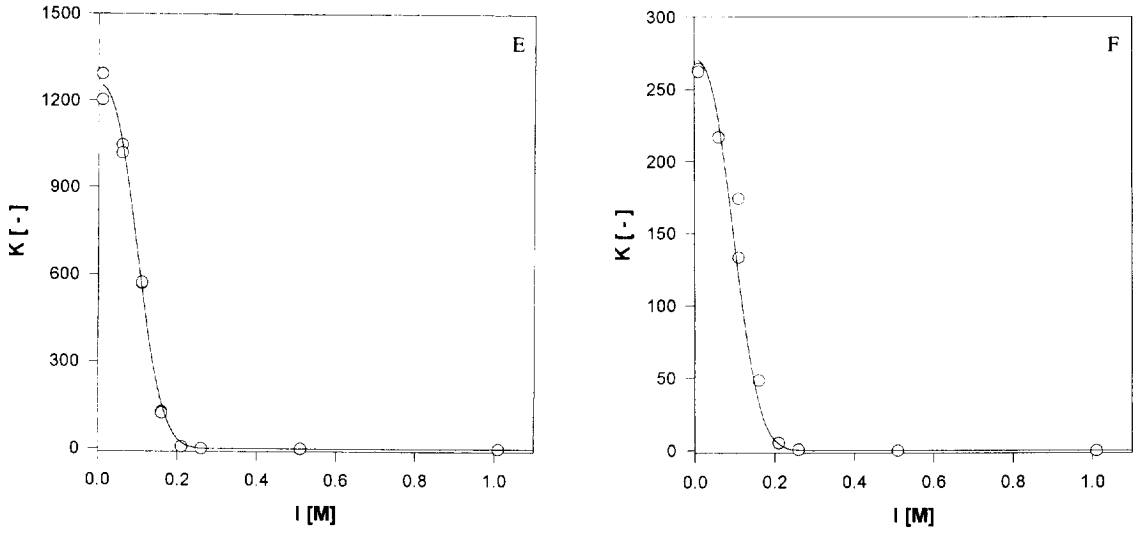

Fig. 5. 2D plots of K values versus protein concentration and salt concentration. Circles indicate experimental data points and lines represent a section of a 3D fit of Eq. A48 to a data set of 94 experimental K values. (A) $I = 0.26$ M; (B) $I = 0.21$ M; (C) $I = 0.16$ M; (D) $I = 0.06$ M; (E) $C = 0.2$ mg BSA/ml; (F) $C = 1.0$ mg BSA/ml.

salt are packed into parameter a, which is related to q_{max}. A q_{max} with a narrow confidence interval does not represent the sole criterion for a good approximation. The coefficient of determination is also a rough measure of the goodness of the fit (Table 2). Other criteria must be chosen for the evaluation of the different equations which we have proposed. These criteria are driven by the intended application of the isotherms. When the isotherm is used for the simulation of the peak profiles, the approximation of K values must be very accurate in the range of salt concentration where the protein has a sufficiently high migration velocity (K is below 5). Further, the equations for the approximations should be as simple as possible. The equations inferred from the first derivative are more complex. As demonstrated in the Results section, these equations have more solutions in the working range (Fig. 4). This can lead to unstable simulation conditions [14,15] unless other sophisticated algorithms are used. Additionally, the approximation becomes very

Table 2
Coefficient of determination (r^2) derived from fit equations, which represent combinations of a number of different adsorption isotherms and different approaches to describe the dependence on the salt concentration (I)

$K(C)$	$K(I)$	Freundlich	Langmuir	Langmuir–Freundlich	Jovanovic	Redlich–Peterson	Toth	Temkin
dC_s/dC_m	LDR	0.99061	0.98858	0.99083	n.f.[a]	0.99084	0.99067	n.f.
dC_s/dC_m	*asym*LDR	0.99616	0.99398	0.99636	n.f.	0.99637	0.99622	n.f.
dC_s/dC_m	tanh	0.99605	0.99387	0.99625	n.f.	0.99625	0.99607	n.f.
dC_s/dC_m	*asym*tanh	0.99696	0.99478	0.99718	n.f.	0.99718	0.99699	n.f.
C_s/C_m	LDR	0.99061	0.99020	0.99101	0.99096	0.99091	0.99195	0.99076
C_s/C_m	*asym*LDR	0.99616	0.99577	0.99616	0.99645	0.99641	0.99688	0.99629
C_s/C_m	tanh	0.99605	0.99566	0.99631	0.99634	0.99620	0.99607	n.f.
C_s/C_m	*asym*tanh	0.99696	0.99665	0.99703	0.99725	0.99722	0.99699	n.f.

[a] n.f. indicates cases where it was not possible to reach a good fit.

sensitive concerning the starting parameters. We do not recommend the use of these equations.

From the results, we conclude that the K value of a protein in an ion exchanger can be expressed by a 3D function. A transition function [logistic dose response (Eq. 3 or 4) or hyperbolic tangent functions (Eq. 5 or 6)] is used for the description of the dependence on salt and conventional adsorption isotherms for the dependences on protein.

Further investigations are in progress to take into account the shapes of the isotherms with increasing salt.

Acknowledgement

We acknowledge the support of BioSepra (Marlborough, MA, USA).

Appendix

Freundlich isotherm

$$C_s = f(C_m) = bC_m^n \tag{A1}$$

For a Freundlich isotherm, the functions derived by a derivatization (dC_s/dC_m) or by a ratio (C_s/C_m) to fit the experimental data are identical, unless the recalculation of parameter b in Eq. A1 is different.

Combination with a logistic dose response function (LDR):

$$\Gamma(I, C_m) = \frac{aC_m^{d-1}}{1+\left(\frac{I}{b}\right)^c} \tag{A2}$$

Combination with an asymmetric logistic dose response function (*asym*LDR):

$$\Gamma(I, C_m) = \frac{aC_m^{d-1}}{\left[1+\left(\frac{I}{b}\right)^c\right]^e} \tag{A3}$$

Combination with a hyperbolic tangent function (tanh):

$$\Gamma(I, C_m) = a \cdot \frac{1+\tanh[-b(I-c)]}{2} \cdot C_m^{d-1} \tag{A4}$$

Combination with an asymmetric hyperbolic tangent function (*asym*tanh):

$$\Gamma(I, C_m)a \cdot \frac{\{1+\tanh[-b(I-c)]\}^e}{2} \cdot C_m^{d-1} \tag{A5}$$

Langmuir isotherm

$$C_s = f(C_m) = q_{max} \cdot \frac{bC_m}{1+bC_m} \tag{A6}$$

Combination of dC_s/dC_m with LDR:

$$\Gamma(I, C_m) = \frac{a}{\left[1+\left(\frac{I}{b}\right)^c\right](1+dC_m)^2} \tag{A7}$$

Combination of dC_s/dC_m with *asym*LDR:

$$\Gamma(I, C_m) = \frac{a}{\left[1+\left(\frac{I}{b}\right)^c\right]^e(1+dC_m)^2} \tag{A8}$$

Combination of dC_s/dC_m with tanh:

$$\Gamma(I, C_m) = \frac{a}{(1+dC_m)^2} \cdot \frac{1+\tanh[-b(I-c)]}{2} \tag{A9}$$

Combination of dC_s/dC_m with *asym*tanh:

$$\Gamma(I, C_m) = \frac{a}{(1+dC_m)^2} \cdot \frac{\{1+\tanh[-b(I-c)]\}^e}{2} \tag{A10}$$

Combination of C_s/C_m with LDR:

$$\Gamma(I, C_m) = \frac{a}{\left[1+\left(\frac{I}{b}\right)^c\right](1+dC_m)} \tag{A11}$$

Combination of C_s/C_m with *asym*LDR:

$$\Gamma(I, C_m) = \frac{a}{\left[1+\left(\frac{I}{b}\right)^c\right]^e(1+dC_m)} \tag{A12}$$

Combination of C_s/C_m with tanh:

$$\Gamma(I, C_m) = \frac{a}{(1+dC_m)} \cdot \frac{1+\tanh[-b(I-c)]}{2} \tag{A13}$$

Combination of C_s/C_m with *asym*tasnh:

$$\Gamma(I, C_m) = \frac{a}{(1 + dC_m)} \cdot \frac{\{1 + \tanh[-b(I - c)]\}^e}{2} \quad \text{(A14)}$$

Langmuir–Freundlich isotherm

$$C_s = f(C_m) = q_{max} \cdot \frac{bC_m^n}{1 + bC_m^n} \quad \text{(A15)}$$

Combination of dC_s/dC_m with LDR:

$$\Gamma(I, C_m) = \frac{aC_m^{e-1}}{\left[1 + \left(\frac{I}{b}\right)^c\right](1 + dC_m^e)^2} \quad \text{(A16)}$$

Combination of dC_s/dC_m with *asym*LDR:

$$\Gamma(I, C_m) = \frac{aC_m^{e-1}}{\left[1 + \left(\frac{I}{b}\right)^c\right]^f (1 + dC_m^e)^2} \quad \text{(A17)}$$

Combination of dC_s/dC_m with tanh:

$$\Gamma(I, C_m) = \frac{aC_m^{e-1}}{(1 + dC_m^e)^2} \cdot \frac{1 + \tanh[-b(I - c)]}{2} \quad \text{(A18)}$$

Combination of dC_s/dC_m with *asym*tanh:

$$\Gamma(I, C_m) = \frac{aC_m^{e-1}}{(1 + dC_m^e)^2} \cdot \frac{\{1 + \tanh[-b(I - c)]\}^f}{2} \quad \text{(A19)}$$

Combination of C_s/C_m with LDR:

$$\Gamma(I, C_m) = \frac{aC_m^{e-1}}{\left[1 + \left(\frac{I}{b}\right)^c\right](1 + dC_m^e)} \quad \text{(A20)}$$

Combination of C_s/C_m with *asyml*LDR:

$$\Gamma(I, C_m) = \frac{aC_m^{e-1}}{\left[1 + \left(\frac{I}{b}\right)^c\right]^f (1 + dC_m^e)} \quad \text{(A21)}$$

Combination of C_s/C_m with tanh:

$$\Gamma(I, C_m) = \frac{aC_m^{e-1}}{(1 + dC_m^e)} \cdot \frac{1 + \tanh[-b(I - c)]}{2} \quad \text{(A22)}$$

Combination of C_s/C_m with *asym*tanh:

$$\Gamma(I, C_m) = \frac{aC_m^{e-1}}{(1 + dC_m^e)} \cdot \frac{\{1 + \tanh[-b(I - c)]\}^f}{2} \quad \text{(A23)}$$

Jovanovic isotherm

$$C_s = f(C_m) = q_{max}[1 - \exp(-bC_m)] \quad \text{(A24)}$$

Combination of dC_s/dC_m with LDR:

$$\Gamma(I, C_m) = \frac{a \exp(-dC_m)}{\left[1 + \left(\frac{I}{b}\right)^c\right]} \quad \text{(A25)}$$

Combination of dC_s/dC_m with *asym*LDR:

$$\Gamma(I, C_m) = \frac{a \exp(-dC_m)}{\left[1 + \left(\frac{I}{b}\right)^c\right]^e} \quad \text{(A26)}$$

Combination of dC_s/dC_m with tanh:

$$\Gamma(I, C_m) = a \cdot \frac{1 + \tanh[-b(I - c)]}{2} \cdot \exp(-dC_m) \quad \text{(A27)}$$

Combination of dC_s/dC_m with *asym*tanh:

$$\Gamma(I, C_m) = a \cdot \frac{\{1 + \tanh[-b(I - c)]\}^e}{2} \cdot \exp(-dC_m) \quad \text{(A28)}$$

Combination of C_s/C_m with LDR:

$$\Gamma(I, C_m) = \frac{a \exp(-dC_m)}{\left[1 + \left(\frac{I}{b}\right)^c\right] C_m} \quad \text{(A29)}$$

Combination of C_s/C_m with *asym*LDR:

$$\Gamma(I, C_m) = \frac{a \exp(-dC_m)}{\left[1 + \left(\frac{I}{b}\right)^c\right]^e C_m} \quad \text{(A30)}$$

Combination of C_s/C_m with tanh:

$$\Gamma(I, C_m) = a \cdot \frac{1 + \tanh[-b(I - c)]}{2} \cdot \frac{\exp(-dC_m)}{C_m} \quad \text{(A31)}$$

Combination of C_s/C_m with *asym*tanh:

$$\Gamma(I, C_m) = a \cdot \frac{\{1 + \tanh[-b(I-c)]\}^e}{2} \cdot \frac{\exp(-dC_m)}{C_m} \quad \text{(A32)}$$

Redlich–Peterson isotherm

$$C_s = f(C_m) = q_{max} \cdot \frac{bC_m}{1 + bC_m^n} \quad \text{(A33)}$$

Combination of dC_s/dC_m with LDR:

$$\Gamma(I, C_m) = \frac{a[1 - (e-1)dC_m^e]}{\left[1 + \left(\frac{I}{b}\right)^c\right](1 + dC_m^e)} \quad \text{(A34)}$$

Combination of dC_s/dC_m with *asym*LDR:

$$\Gamma(I, C_m) = \frac{a[1 - (e-1)dC_m^e]}{\left[1 + \left(\frac{I}{b}\right)^c\right]^f (1 + dC_m^e)} \quad \text{(A35)}$$

Combination of dC_s/dC_m with tanh:

$$\Gamma(I, C_m) = a \cdot \frac{1 + \tanh[-b(I-c)]}{2} \cdot \frac{[1 - (e-1)dC_m^e]}{(1 + dC_m^e)} \quad \text{(A36)}$$

Combination of dC_s/dC_m with *asym*tanh:

$$\Gamma(I, C_m) = a \cdot \frac{\{1 + \tanh[-b(I-c)]\}^f}{2} \cdot \frac{[1 - (e-1)dC_m^e]}{(1 + dC_m^e)} \quad \text{(A37)}$$

Combination of C_s/C_m with LDR:

$$\Gamma(I, C_m) = \frac{a}{\left[1 + \left(\frac{I}{b}\right)^c\right](1 + dC_m^e)} \quad \text{(A38)}$$

Combination of C_s/C_m with *asym*LDR:

$$\Gamma(I, C_m) = \frac{a}{\left[1 + \left(\frac{I}{b}\right)^c\right]^f (1 + dC_m^e)} \quad \text{(A39)}$$

Combination of C_s/C_m with tanh:

$$\Gamma(I, C_m) = \frac{a}{(1 + dC_m^e)} \cdot \frac{1 + \tanh[-b(I-c)]}{2} \quad \text{(A40)}$$

Combination of C_s/C_m with *asym*tanh:

$$\Gamma(I, C_m) = \frac{a}{(1 + dC_m^e)} \cdot \frac{\{1 + \tanh[-b(I-c)]\}^f}{2} \quad \text{(A41)}$$

Toth isotherm

$$C_s = f(C_m) = q_{max} \cdot \frac{C_m}{(b + C_m^n)^{1/n}} \quad \text{(A42)}$$

Combination of dC_s/dC_m with LDR:

$$\Gamma(I, C_m) = \frac{a(d + C_m^e)^{-(1+1/e)}}{\left[1 + \left(\frac{I}{b}\right)^c\right]} \quad \text{(A43)}$$

Combination of dC_s/dC_m with *asym*LDR:

$$\Gamma(I, C_m) = \frac{a(d + C_m^e)^{-(1+1/e)}}{\left[1 + \left(\frac{I}{b}\right)^c\right]^f} \quad \text{(A44)}$$

Combination of dC_s/dC_m with tanh:

$$\Gamma(I, C_m) = a \cdot \frac{1 + \tanh[-b(I-c)]}{2} \cdot (d + C_m^e)^{-(1+1/e)} \quad \text{(A45)}$$

Combination of dC_s/dC_m with *asym*tanh:

$$\Gamma(I, C_m) = a \cdot \frac{\{1 + \tanh[-b(I-c)]\}^f}{2} \cdot (d + C_m^e)^{-(1+1/e)} \quad \text{(A46)}$$

Combination of C_s/C_m with LDR:

$$\Gamma(I, C_m) = \frac{a}{\left[1 + \left(\frac{I}{b}\right)^c\right](d + C_m^e)^{1/e}} \quad \text{(A47)}$$

Combination of C_s/C_m with *asym*LDR:

$$\Gamma(I, C_m) = \frac{a}{\left[1 + \left(\frac{I}{b}\right)^c\right]^f (d + C_m^e)^{1/e}} \quad \text{(A48)}$$

Combination of C_s/C_m with tanh:

$$\Gamma(I, C_m) = \frac{a}{(d + C_m^e)^{1/e}} \cdot \frac{1 + \tanh[-b(I-c)]}{2} \quad \text{(A49)}$$

Combination of C_s/C_m with *asym*tanh:

$$\Gamma(I, C_m) = \frac{a}{(d + C_m^e)^{1/e}} \cdot \frac{\{1 + \tanh[-b(I-c)]\}^f}{2} \quad \text{(A50)}$$

Temkin isotherm

$$C_s = f(C_m) = \frac{a}{n} \cdot \ln\left[\frac{1 + bC_m}{1 + \exp(-n)bC_m}\right] \quad \text{(A51)}$$

Combination of dC_s/dC_m with LDR:

$$\Gamma(I, C_m) = \frac{a}{\left[1 + \left(\frac{I}{b}\right)^c\right](1 - dC_m)(dC_m + e)} \quad \text{(A52)}$$

Combination of dC_s/dC_m with *asym*LDR:

$$\Gamma(I, C_m) = \frac{a}{\left[1 + \left(\frac{I}{b}\right)^c\right]^f (1 - dC_m)(dC_m + e)} \quad \text{(A53)}$$

Combination of dC_s/dC_m with tanh:

$$\Gamma(I, C_m) = \frac{a}{(1 - dC_m)(dC_m + e)} \cdot \frac{1 + \tanh[-b(I-c)]}{2} \quad \text{(A54)}$$

Combination of dC_s/dC_m with *asym*tanh:

$$\Gamma(I, C_m) = \frac{a}{(1 - dC_m)(dC_m + e)} \cdot \frac{\{1 + \tanh[-b(I-c)]\}^f}{2} \quad \text{(A55)}$$

Combination of C_s/C_m with LDR:

$$\Gamma(I, C_m) = \frac{a}{\left[1 + \left(\frac{I}{b}\right)^c\right]C_m} \cdot \ln\left(\frac{1 + dC_m}{1 + eC_m}\right) \quad \text{(A56)}$$

Combination of C_s/C_m with *asym*LDR:

$$\Gamma(I, C_m) = \frac{a}{\left[1 + \left(\frac{I}{b}\right)^c\right]^f C_m} \cdot \ln\left(\frac{1 + dC_m}{1 + eC_m}\right) \quad \text{(A57)}$$

Combination of C_s/C_m with tanh:

$$\Gamma(I, C_m) = \frac{a}{C_m} \cdot \frac{1 + \tanh[-b(I-c)]}{2} \cdot \ln\left(\frac{1 + dC_m}{1 + eC_m}\right) \quad \text{(A58)}$$

Combination of C_s/C_m with *asym*tanh:

$$\Gamma(I, C_m) = \frac{a}{C_m} \cdot \frac{\{1 + \tanh[-b(I-c)]\}^f}{2} \cdot \ln\left(\frac{1 + dC_m}{1 + eC_m}\right) \quad \text{(A59)}$$

References

[1] H. Freundlich, Phys. Chem., 57 (1907) 385.
[2] I. Langmuir, J. Am. Chem. Soc., 40 (1918) 1361.
[3] R. Sips, J. Chem. Phys., 16 (1948) 490.
[4] O. Redlich and D. Peterson, J. Phys. Chem., 63 (1959) 1024.
[5] J. Huang and C. Horvath, J. Chromatogr., 406 (1987) 275.
[6] J. Huang and C. Horvath, J. Chromatogr., 406 (1987) 285.
[7] M.I. Temkin, Zh. Fiz. Khim., 14 (1940) 1153.
[8] J. Toth, J. Colloid Interface Sci., 79 (1981) 85.
[9] L. Jossens, J.M. Prausnitz, W. Fritz, E.U. Schlünder and A.L. Myers, Chem. Eng. Sci., 33 (1978) 1097.
[10] J.C. Bellot and J.S. Conderet, J. Chromatogr., 635 (1993) 1.
[11] S. Yamamoto, K. Nakanishi and R. Matsuno, Ion-Exchange Chromatography of Proteins, Marcel Dekker, New York, 1988.
[12] A. Velayudhan and Cs. Horvath, J. Chromatogr., 443 (1988) 13.
[13] A. Jungbauer and O. Kaltenbrunner, Biotechnol. Bioeng., in press.
[14] M. Czok and G. Guiochon, J. Chromatogr., 537 (1991) 497.
[15] L.R. Snyder and G.B. Cox, J. Chromatogr., 537 (1991) 507.